N O T I C E

THIS DOCUMENT HAS BEEN REPRODUCED FROM MICROFICHE. ALTHOUGH IT IS RECOGNIZED THAT CERTAIN PORTIONS ARE ILLEGIBLE, IT IS BEING RELEASED IN THE INTEREST OF MAKING AVAILABLE AS MUCH INFORMATION AS POSSIBLE

MCR-81-576

NASA CR-166731

Volume I

Executive Summary

May 1981

Onboard Utilization of Ground Control Points for Image Correction Final Report

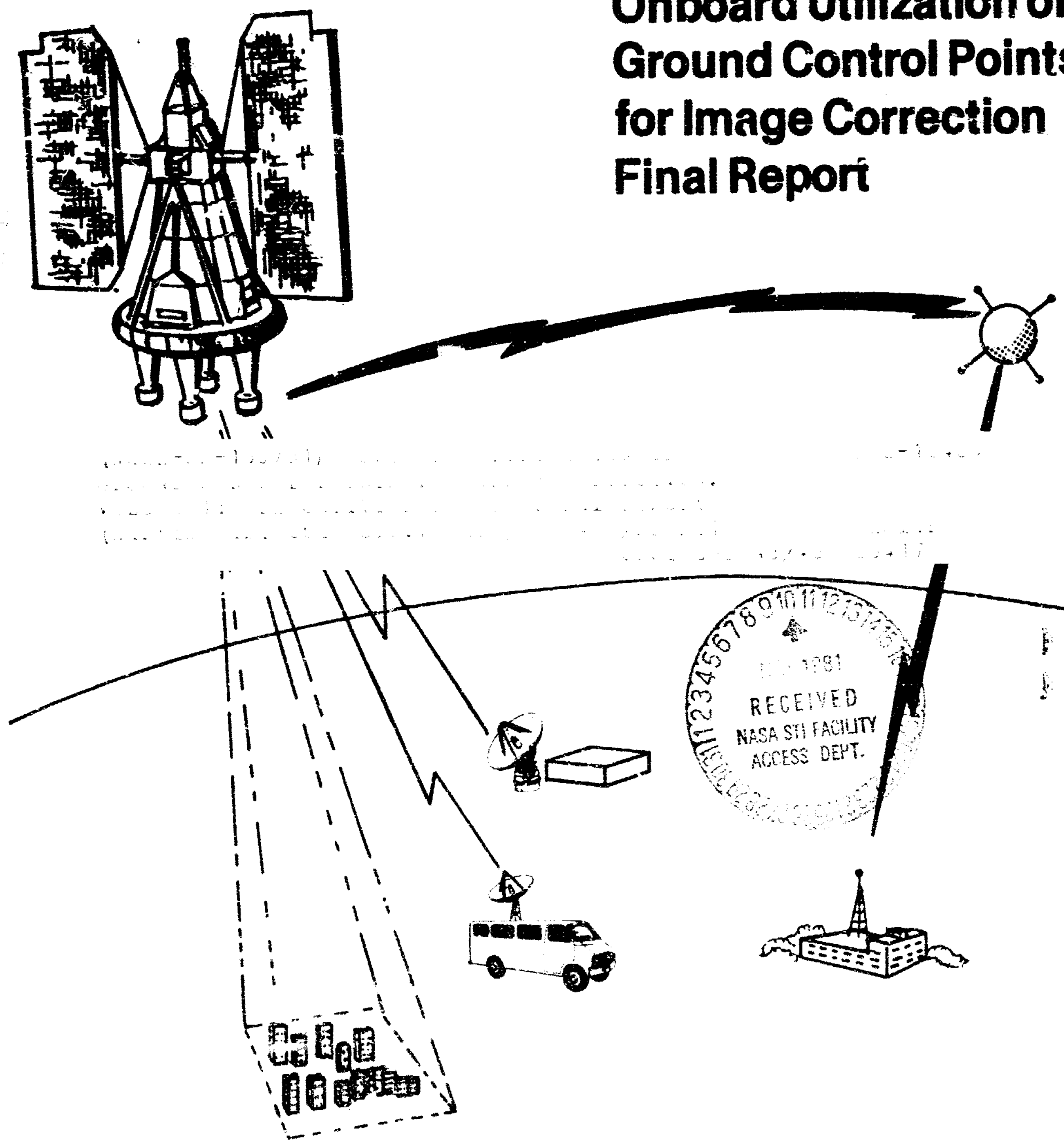

RECEIVED
NASA STI FACILITY
ACCESS DEPT.

MARTIN MARIETTA

I FOREWORD

This volume of the "Onboard Utilization of Ground Control Points for Image Correction" final report provides an executive summary of the study and simulation results and includes our recommendations relating to future mission requirements.

Three other volumes have been incorporated into the final report. Volume II provides a detailed description of the study and simulation results, and Volumes III and IV are appendices containing a description of all software designed and utilized under this contract.

II. INTRODUCTION

Several current and anticipated trends threaten to limit the usefulness of future NASA remote sensing missions if we continue to employ current data handling methods. Forecasts of instrumentation trends show an increase in sensor resolution from 80 meters for Landsat 1 to 15 meters for the Operational Earth Resources Satellite (OERS) planned for launch in 1990 (Ref 1). In addition to the increased resolution, the OERS design currently calls for 20 different bands. This translates to an increase in total data rates for earth sensing missions from 1 million bits per second (Mbps) to over 100 Mbps; an increase of two orders of magnitude in less than five years. In addition to affecting the data rates, increased sensor resolution affects the following areas:

- o Greater processing requirements for image correction, formatting, and information extraction.
- o Increased navagation accuracy requirements to provide the necessary image distortion coefficients.
- o Increased archiving requirements to accept the larger data volume.

Increased resolution of the science sensor is a positive trend for applications. However, the acquisition of these data is totally non-deterministic in that nothing is known about the quality, content, or location of the imagery prior to or even shortly after it is obtained. As a result very little of the information is used by the scientific community because of such undesirable effects as cloud coverage, unwanted scene content, or exposure dates that do not coincide with those desired. In fact, less than 1% of all previously acquired remotely sensed data have been processed by the user.

In addition to the data deluge problem, it is currently not feasible to exploit Landsat data for such real-time applications as forest fire detection and monitoring and flood detection. In fact, with the exception of applications in which the observables do not change dramatically with time (such as oil exploration), Landsat's usefulness is limited from an operational standpoint because the data are already stale by the time the user gets them.

User requirements are another important trend associated with remote sensing missions because in the long run these requirements play a major role in defining the mission. Current data dissemination techniques are limited to a several-month turnaround. However, many users require this time to be cut to hours, and a set of future users are requesting real-time control of the science instrument. The primary limiting factor in data turnaround time is the processing required for image registration. The impact of non deterministic data acquisition is that excessive processing is required to handle these data and register unwanted scenes. Excessive processing leads to both rising support costs and unacceptable data turnaround.

The final trend that must be overcome to realize future missions is the rapidly escalating cost of ground support. The primary drivers of this trend are manpower costs and sophisticated equipment.
A detailed examination of the problem reveals that the following areas are the most critical limitations of current remote sensing missions.

- Remote sensing missions do not employ any automated techniques of data evaluation for either simple annotation or data negation. A simple determination of percentage cloud coverage in a scene could effectively eliminate on the order of 50% of the data acquired.

- Users are subject to the schedule of the mission rather than the mission being tailored to the specific acquisition requirements of the user. This results in the acquisition of tremendous volumes of unwanted imagery either due to poor quality caused by atmospheric effects, the geographic location, or the time of acquisition. Also, if a user schedules an experiment around the Landsat schedule and weather effects are undesirable for that period of time, it is either necessary to wait eight days for the next Landsat overflight or delete remotely sensed data from the experimental requirements. Unfortunately this happens all too often.

- All data, including tracking data from remote stations, must be sent to a central facility for image correction, annotation, and packetization, and then sent to a second facility for archiving and eventual dissemination to the users. This results in an unnecessary data link and awkward procedures to ensure critical timing requirements are met. This process is neither cost nor time effective.

- No advantage is being taken of the onboard navigation capability to limit the magnitude of image distortions. By providing onboard control, the magnitude of the processing involved can be dramatically reduced.

The purpose of this contract was to investigate a new approach to remote sensing that would meet future mission requirements by overcoming these problems.

The primary sources of image distortion are sensor-peculiar errors, viewing perspective, coordinate transformation errors, and spacecraft-induced errors. With the development of the multilinear array, the primary sensor-caused distortions will be the individual placement of the detector elements, optical effects, and orientation of the array relative to the sensor coordinate frame prior to flight. These errors remain fairly constant over time so the resulting distortions are deterministic. In referring to Figure II-1, viewing perspective is a well-known function of local earth radius and vehicle altitude and can be computed as shown.

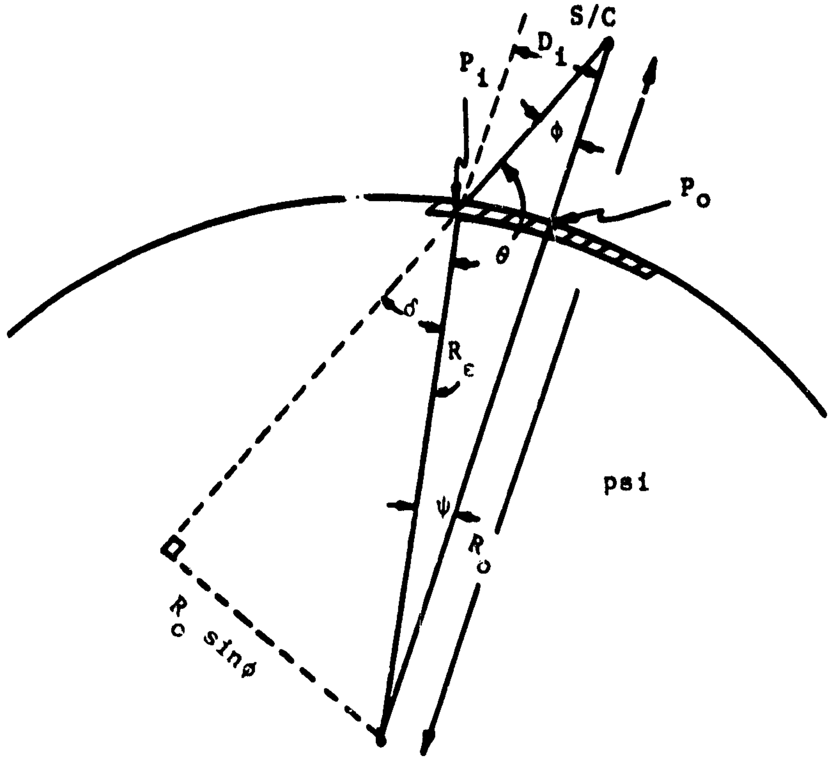

where

$$\delta = \sin^{-1} \frac{R_o \sin\phi}{R_\varepsilon}$$

$$\theta = 180 - \delta$$

$$\psi = 180-(\theta + \phi) = \sin^{-1} \frac{R_o \sin\phi}{R_\varepsilon} - \theta$$

D_i = surface distance of i^{th} element from the center of the field of view = ψR_ε,

R_i = effective resolution of i^{th} element = $D_i - D_{i-1}$

distortion of i^{th} pixel = $R_i - R_{ref}$

where R_{ref} is the desired resolution.

Figure II-1 Viewing Perspective Distortions

It is assumed that the local earth radius is known so this distortion is also deterministic. The primary error source remaining, therefore, is spacecraft-induced. The spacecraft error sources can be categorized as:

1) Attitude determination,
   a) Star tracker accuracy,
   b) Star tracker configuration,
   c) Knowledge of star tracker misalignment,
   d) Error in star catalog,
   e) Gyro noise,
   f) Uncertainty in gyro bias, nonorthoganality and misalignment,
   g) Numerical accuracy;
2) Ephemeris prediction,
   a) Global positioning system (GPS) accuracy,
   b) Dynamic model accuracy,
   c) GPS update interval,
   d) Numerical accuracy;
3) Transformation error between inertial and earth-fixed coordinates,
   a) Knowledge of UTI,
   b) Knowledge of earth preccession, nutation, polar wander, and tidal deformation,
   c) Numerical accuracy;
4) Misalignment between sensor and body coordinates,
   a) Knowledge of linear array orientation,
   b) Accuracy of thermal distortion model,
   c) Vibration modes between two coordinates,
   d) Calibration technique and frequency,
   e) Numerical accuracy.

For the sake of discussion, assume that all the error is due simply to the attitude determination system. To achieve the temporal registration requirement of 15 meters, it will be necessary to predict attitude to within 4 arc seconds as illustrated in Figure I-2. The accuracy of the state-of-the-art systems using the NASA standard star tracker and gyro is 15 arc-seconds (2σ) (Ref 2).

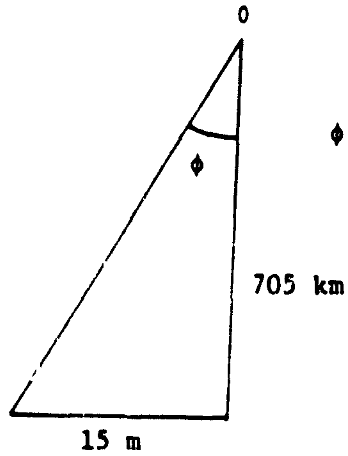

$$\phi = \tan^{-1} \frac{15 \text{ m}}{705 \text{ km}}$$
$$= 4 \text{ s}$$

Figure II-2 Error Budget for Registration Accuracy of 15 m

Even with the development of charge-coupled device (CCD) star trackers, the attitude determination capability will be around 6 arc seconds (2σ). Note that 2σ numbers have been used here corresponding to 95% of the data. If 1σ numbers corresponding to 67% of the data are used, the accuracy goals can be met. However, by adding even one more error term such as misalignment between sensor and body coordinates of 2 arc seconds (2-axis alignment accuracy achievable with optical alignment cubes), the total error budget is exceeded. From the previous discussion, which ignored many error sources, it is clear that another approach is required.

The key to real-time image correction lies in being able to accurately determine the location of the science sensor's boresight in earth-fixed coordinates. With this capability it is not only possible to provide real-time measurements of the image distortions, but with the advent of the multilinear array (MLA) it may be possible to provide real-time image correction using either resampling or special design of the MLA focal plane. This capability also provides the heart of a pointing system capable of deterministically acquiring imagery at specific earth-fixed coordinates.

Shortly after definition of the feature identification and location experiment (FILE), Martin Marietta began the development of a landmark tracker or GCP detector centered around experience gained with terminal guidance systems. The primary purpose of the landmark tracker is to provide periodic measurements of the science sensor's boresight position to be used as input to a navigation system. Previous studies (Ref 4 thru 7) have shown that the landmark tracker cannot solve for both position and attitude without supplemental measurements from another source. Another limitation of the landmark tracker operating in the visible spectrum is that observations can be obscured by clouds and the correlator will lock onto a false target. For these reasons the conceptual navigation system consists of the landmark tracker, a GPS receiver, and two NASA standard star trackers to replace attitude measurements when the landmark is obscured.

The purpose of this contract was to simulate operation of a navigation system centered around image correction, and analyze performance of the system under a variety of conditions. Also of interest was a sensitivity analysis to determine the optimal sampling interval for each sensor, and the total number of landmarks required to satisfy mission requirements.

III. ONBOARD IMAGE CORRECTION SYSTEM OVERVIEW

The onboard image correction system has been separated into three primary subsystems as illustrated in Figure III-1. The navigation processor accepts measurements from the GPS receiver, the star trackers, and the landmark tracker, and solves for spacecraft state. The registration processor is responsible for correlating live imagery with stored reference ground control points to produce a landmark sighting vector. This processor is also responsible for providing measurements of the distortion coefficients, and for providing image resampling if this operation is performed on board. The pointing mount controller is used to isolate the sensor from the attitude limit cycle and to provide additional flexibility through sensor pointing.

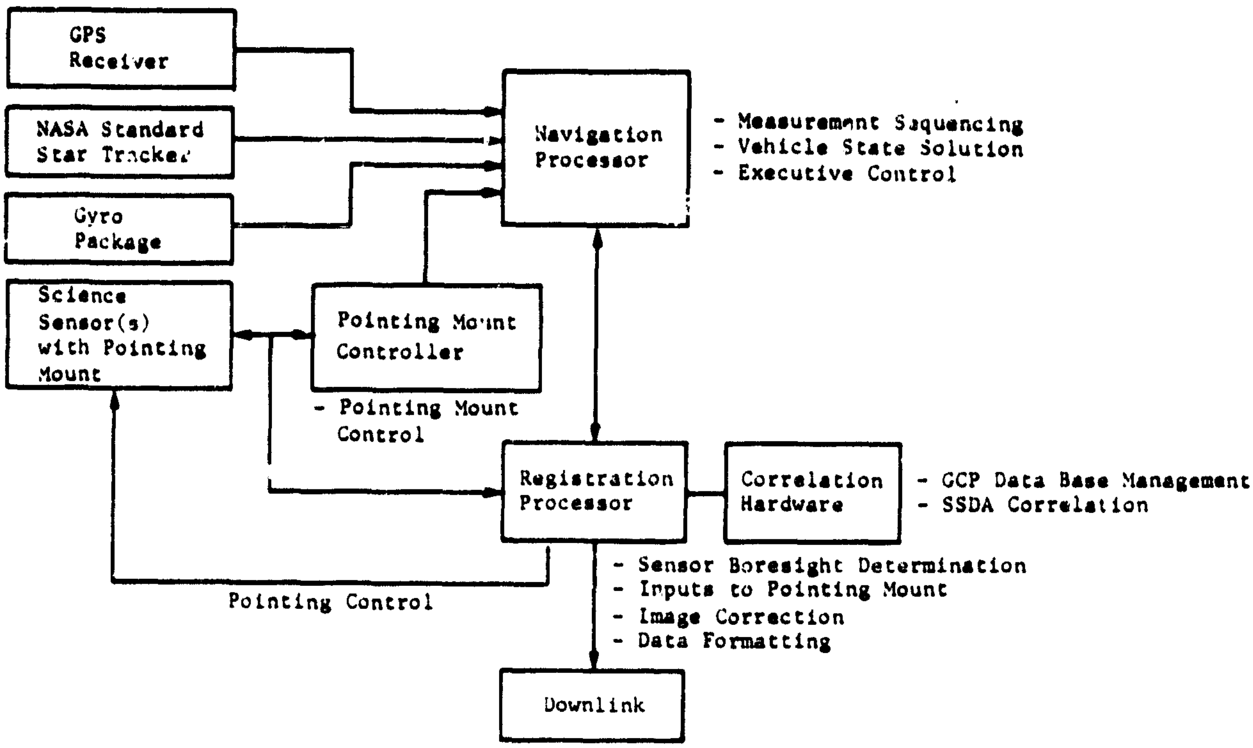

Figure III-1 Onboard Image Correction System Block Diagram

A. REGISTRATION PROCESSOR

Figure III-2 illustrates the functional flow of the registration processor. A digital representation of all the ground control points is stored on a high-density tape recorder (or bubble memory) and read into random access memory as required. Because of the reliability considerations associated with the recorder, a number of GCPs will be read into RAM at one time. As the spacecraft proceeds in orbit, the landmark that is to be viewed next is determined and the digital reference image is extracted from RAM. Information stored in the GCP file, along with uncertainty in vehicle position and attitude, helps to define the location and size of the search area. For an operational system it is advisable to use a fixed-size search area. Since a star tracker is being used for backup, the maximum attitude error will be in the vicinity of 15 arc seconds (2σ) and the global positioning system will produce an error around 12 meters. Therefore a search area that is 32 pixels larger than the GCP size will provide far more area than required. For this reason, and the fact that a GCP size of 32 produces the best results, a search area size of 64 was chosen.

Proceeding with registration processing, a test is initiated to determine if the location of the present scan line is coincident with the position of the search area. If it is not, a new satellite state is obtained from the navigation processor. This new state is then transformed into sensor pointing information for use by the pointing mount controller. In the normal mode of operation, the pointing mount controller uses gyro data to compensate for the attitude limit cycle thus reducing the magnitude of the distortions. If the pointing mount is being used to provide deterministic data acquisition according to earth-fixed coordinates, the boresight position provided by the registration processor will also be used as a reference to point from. Following the determination of boresight position, the loop continues until the current scan line is coincident with the search area.

At this point, image scan lines extracted from the sensor are stored in a buffer and become the search area data. The search area is then registered with respect to the GCP and the registration vector passed to the navigation processor, which uses this information to update the estimate of vehicle state. The entire process is then repeated for the next landmark.

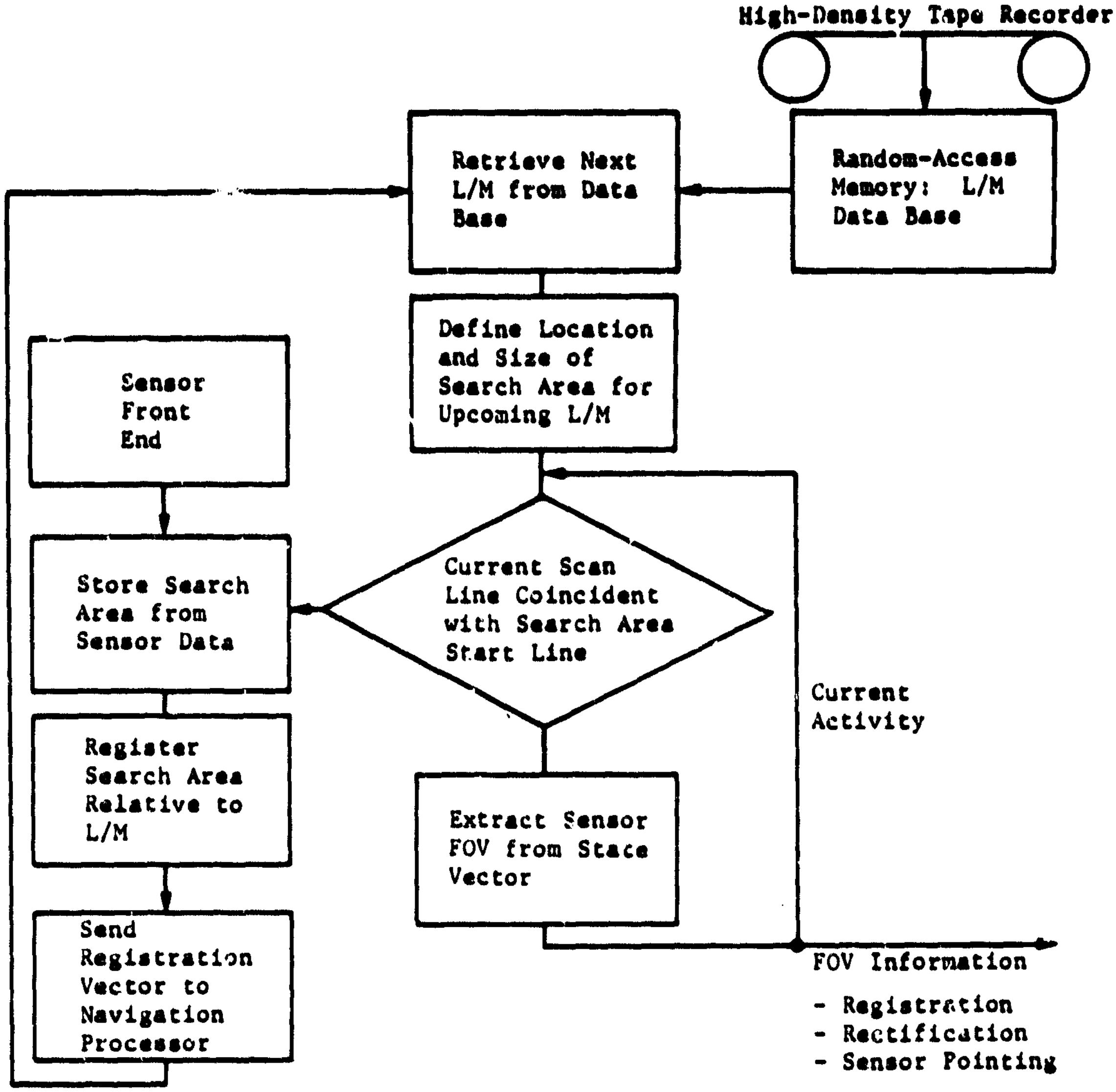

Figure III-2 Functional Flow of Registration Processor

B. NAVIGATION PROCESSOR

Figure III-3 illustrates the functional processing performed by the navigation processor. The most critical function performed is the sequencing of measurements and supervisory control of the registration processor. The sequencer first decides, based on a measurement profile, what type of measurement should be made and when the measurement should be made. The types of measurements the sequence tables establish are star trackers 1 and 2 and GPS. After determining the time of the next measurement, the sequencer decides, based on the total number of scan lines left to the landmark and the scan rate of the sensor, whether there is enough time before the landmark sighting. If there is, the measurement is processed normally. If there is not, control is defaulted to the registration processor until the registration vector if returned.

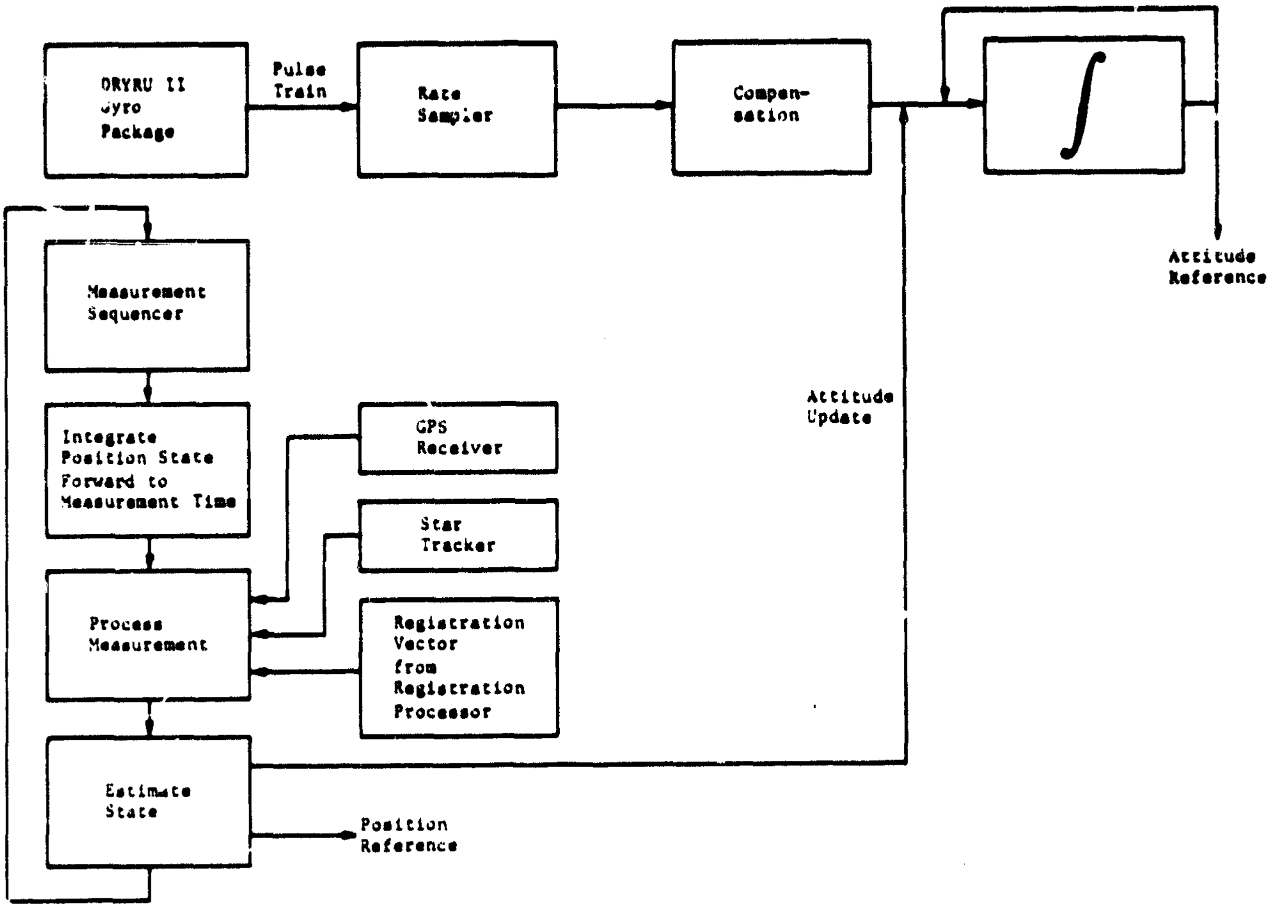

Figure III-3 Navigation Processor Functional Description

After the measurement is obtained, the estimated state vector is intergrated forward to the measurement time. This process is part of the extended square root navigation filter but is implemented in a separate package to simplify control. The raw measurements are processed to compensate for knowledge of such error terms as bias and misalignment. These compensated measurements are used as input to the Kalman filter package that then estimates the spacecraft state. The spacecraft state includes:

1) Position;

2) Velocity;

3) Attitude;

4) Gyro drift, nonorthoganality, and scale factor;

5) Science sensor misalignment.

The navigation processor is responsible for sending the navigation state to the registration processor at the beginning of each scan line. This information is used to compute the distortion coefficients and to control the sensor pointing mount. Attitude is propagated between measurements by a NASA standard gyro package. The pulse train output from the gyros is compensated for knowledge of bias, nonorthogonality, and scale factor and then integrated to provide vehicle attitude.

C. POINTING MOUNT CONTROLLER AND LINEAR ARRAY

The pointing mount controller can be implemented in two different ways, depending on the configuration of the image correction system. If a curved focal plane array is used, the pointing mount controller would be responsible for maintaining the boresight of the instrument along nadir. In a system where image correction is provided through resampling, the pointing mount controller could be used to provide deterministic data acquisition by pointing to specified earth-fixed coordinates.

In a curved focal plane configuration, the pointing mount controller would form an error vector that represents the angular offset between the boresight of the linear array and nadir. This error vector would then be used as an input to the pointing mount to correct for the error. In this way the viewing angle of the MLA would be isolated from the spacecraft motion caused by either attitude limit cycles or attitude corrections.

In a selective acquisition mode the sensor boresight position would be compared to the desired pointing angle to generate an offset that would be used as an input to the positioning mount. Again the viewing angle of the sensor can be isolated from the spacecraft motion to simplify the image correction process.

The idea behind a curved focal plane array originates from the understanding that, with the development of the MLA, the primary image distortions will be caused by the viewing angle and the curvature of the earth (Fig. II-1). This nonuniform sampling is relatively constant and is symmetrical about a vector pointing along nadir. It was therefore felt that constructing an array with nonuniform sampling for each element that compensated for these effects could eliminate along scan resampling, which is one of the largest bottlenecks of remote sensing (Figure III-4).

The limitations of this approach are that the central element must always point at nadir to within 0.5 the resolution angle of the sensor. While this is anticipated as being feasible with either Gimbalflex or the angular suspension pointing system, a constraint is placed on the system in that it can no longer be used for deterministic data acquisition through sensor pointing. On the other hand, the cost savings and increased data turnaround time make this an attractive possibility that warrants further investigation. The key considerations that need to be addressed are:

1) Can the curvature of the focal plane maintain a precision that ensures additional distortions are not introduced?

2) Is the variation in the local curvature of earth great enough to introduce errors greater than 0.5 pixel?

3) Are variations in the orbital altitude great enough to cause distortions?

4) What is the cost savings of performing real-time image correction using this technique versus complex resampling processors.

5) How real is the desire to provide deterministic data acquisition through sensor pointing? Are the cost savings of deterministic data acquisition greater than the cost of producing the curved focal plane array? Can the severe distortions introduced by pointing 30° off axis be corrected?

The answers to these questions will form the basis for selecting the system architecture to be used on the next generation of remote sensing vehicles. However, even if a curved focal plane is not chosen, the separation of the science instrument from the motion of the spacecraft through the use of a pointing mount will reduce the distortions and simplify the process of image correction while providing deterministic data acquisition.

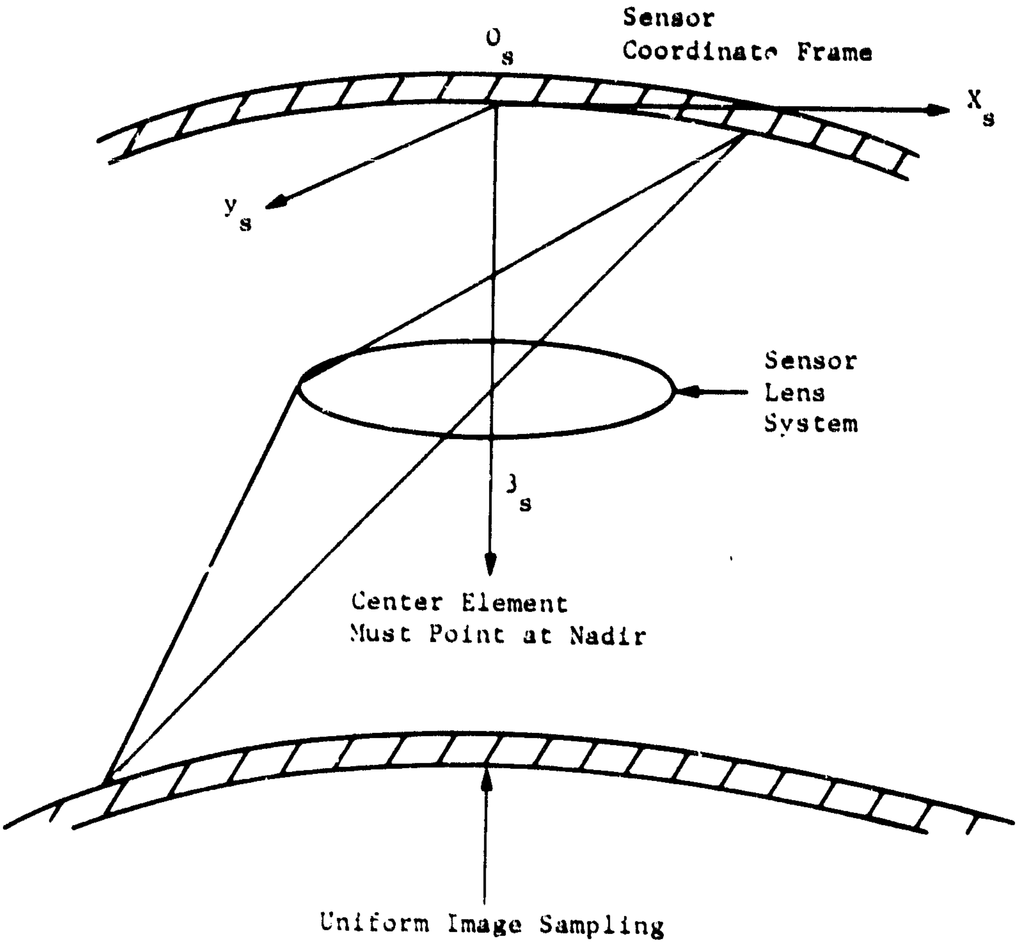

Figure III-4 Curved Focal Plan Array

IV. GCP NAVIGATION SYSTEM SIMULATION

The GCPSIM program has been configured to provide scientific simulations to predict the performance of the GCP detection system. Two types of simulation modes have been incorporated. The first mode simulates the spacecraft, the spacecraft environment and all measurements. The second mode extracts ground control point measurements directly from Landsat imagery.

The program was set up to provide extensive error analysis rather than simply a convariance analysis. Although a convariance analysis provides a great deal of information, in many cases this information can be inaccurate or misleading. For example, there are cases where the covariance matrix converges over a period of time while the actual state estimate diverges from the true state. For this reason the simulation models the true state of the vehicle using the dynamic equations of motion. By propagating the true vehicle state, one can perform a covariance analysis and also generate the actual state error and measurement residuals.

A. SIMULATED GCP MEASUREMENT

GCPSIM was designed to provide the ability to analyze the effect of various measurement sequences. This was particularly important when studying the effect of GCP spacing, missed GCP sightings, and the expected accuracy after traversing a large body of water. The measurement sequencer designed for GCPSIM allows any mixture of GCP, global positioning system, or star tracker measurements and time delays (periods during which no measurements were made) of any length. The sequencer determines the type of measurement and the time at which the measurement should be made. The true vehicle position state is then propagated forward to this time by integrating the nonlinear equations of motion with some additional process noise to account for modeling errors. The attitude state is propagated by looking up the body rates in an attitude profile table and integrating these rates.

The true vehicle state is used along with a measurement model to generate an ideal measurement vector. The ideal measurement is then corrupted with noise, bias, and misalignment terms and compensated for knowledge of these values. This allows a careful analysis of the effect of misalignment on the state solution. It is important to understand the effect of bias and misalignment between the landmark tracker and body axis because this is the largest unknown factor contributing to a pointing error. It is possible to provide frequent calibration for these misalignment errors, but it is difficult to model, for any length of time, the various processes that cause the misalignment. For example, thermal gradients across the vehicle and vibrational modes within the flexible structure are complex functions of such things as structural design, sun angle, physical properties of the material and many other factors. These processes are the most difficult and least understood of all engineering problems.

The compensated measurements are used as inputs into an extended square root Kalman filter, which estimates the true vehicle state. The extended filter propagates the estimated navigation state, the state transition matrix and the process noise array between measurements by integrating the various differential equations using a fourth-order Runge Kutta Gill process. The estimated attitude state is propagated by a gyro model that corrupts the output with gyro drift, noise, non-orthogonality, scale factor and misalignment. The gyro output is compensated in a similar fashion to the measurement model.

The estimated state is used to form an estimated measurement, which in turn is subtracted from the true measurement to obtain a residual. The measurement residual and calculated Kalman gain are used to update the state estimate, which can be compared with the true state to yield the state error. The entire process continues until the spacecraft is propagated forward to the run stop time.

1. Measurement Models

The types of measurements modeled in GCPSIM include GPS position and velocity, star tracker sightings, and landmark tracker sightings. The design philosophy behind the measurement models is that the actual vehicle state is used with a geometry model to yield an ideal measurement vector. This ideal vector is then corrupted with bias, noise, and misalignment to provide the actual sensor output. The sensor output is compensated for some estimate of the error terms and is then used by the filter to estimate the vehicle state. The benefit this design approach provides is that it allows a detailed analysis of sensitivity to misalignments and compensation ability. A functional description of the measurement models is provided in Figure IV-1.

2. Dynamics Model and Navigation State Integrator

The dynamics model and state integrator are very closely related in that the dynamics model calculates the values of the differential equation that is used by the integrator. For this reason, the two are discussed together in this section.

a. Dynamics Model - The dynamics model calculates the derivative of the spacecraft navigational state, which will be integrated to produce the navigational state vector. This is done in part by calculating the total acceleration of the spacecraft due to solar pressure and gravitation effects of the sun, moon, and earth, including fourth zonal harmonic terms.

The sequential process for determing the forces acting on the spacecraft is:

1) Calculate Julian data;
2) Calculate solar and lunar positions;
3) Calculate solar pressure acceleration;
4) Calculate gravitational acceleration due to sun and moon;
5) Calculate gravitational acceleration due to earth using four zonal harmonic terms;
6) Calculate total acceleration.

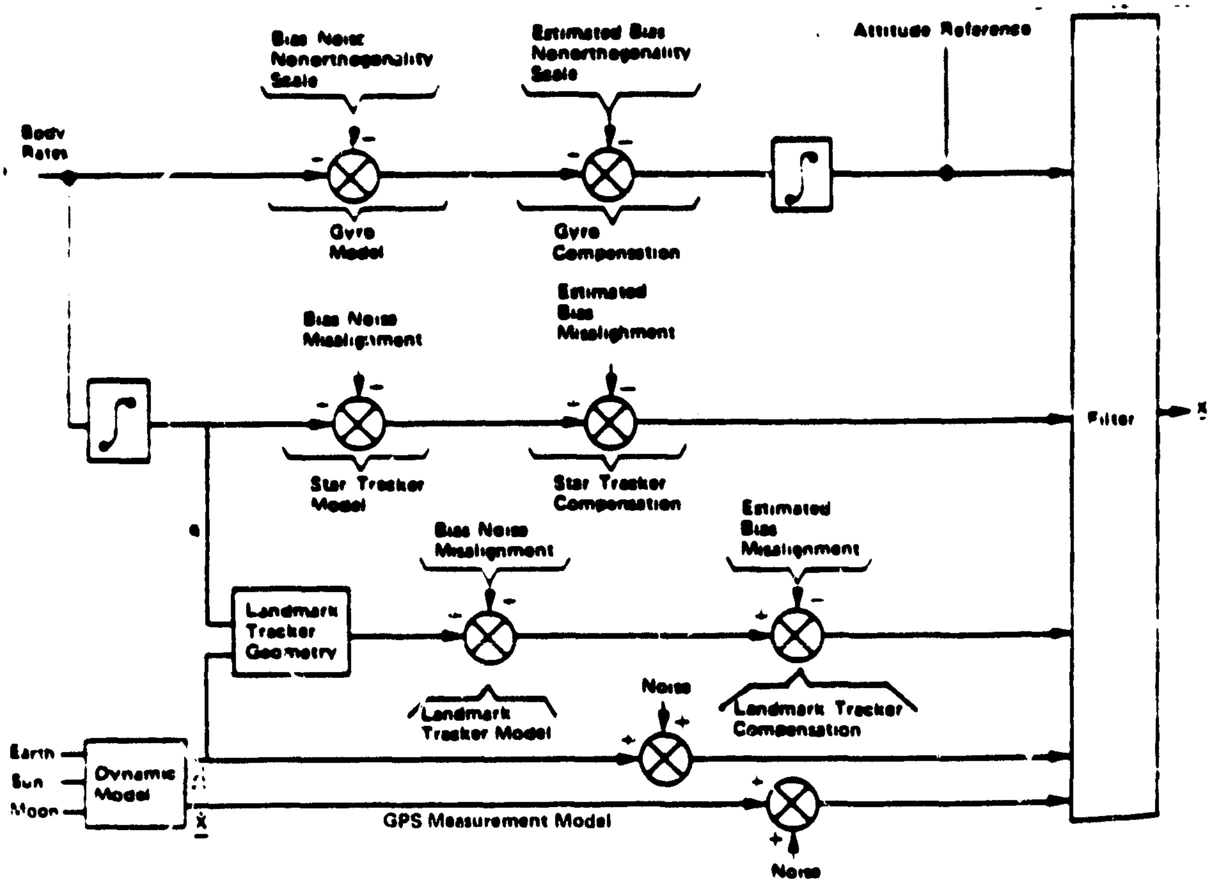

Figure IV-1 Overview of Measurement Models

b. <u>Navigation State Integrator</u> - The position state is advanced in time by numerical integration of the equations of motion. The second-order equations of motion are composed of the external forces acting on the spacecraft. The external forces consist of geopotential, lunar and solar gravitation, and radiation pressure. The integration routine is used to propagate both the actual state and the estimated state between measurement times. A study showed that the Runge Kutta Gill (RKG) fourth-order numerical integration method is optimal for this application. It is self-starting, handles variable step sizes, and is sufficiently accurate.

3. <u>The Extended Carlson Square Root Filter Mechanization</u>

The Carlson square root filter that was mechanized in GCPSIM is an extension of the conventional Kalman filter where the optimal gain, state and covariance updates are determined using a matrix that is the square root of the conventional covariance matrix. The advantages of this mechanization are higher accuracy for a given machine precision and a guaranteed positive covariance. The extended filter is necessary due to the nonlinear nature of the process. The filter propagages the state, state transition, and process noise covariance by integration of differential equations rather than linear propagation over the appropriate intervals.

The sequence process used in the navigation filter is:

1) Integrate state to measurement time
2) Integrate state transition matrix to measurement time
3) Integrate process noise to measurement time
4) Propagate covariance matrix to measurement time using state transition matrix
5) Decompose covariance matrix to its square root form
6) Generate measurement residual
7) Compute Kalman gain
8) Update state

B. EXTRACTED GCP MEASUREMENTS

The second mode of operation allowed by GCPSIM provides for a mixture of modeled and actual measurements. The GPS and star tracker measurements are modeled as discussed previously. The GCP measurements, however, are extracted from actual imagery obtained from Landsat.

The second mode of operation functions much the same way as the first mode. The sequencer defines the type and time of the star tracker and GPS measurements. The GCP data base containing the number of scan lines to the next GCP is consulted to see if the GCP will be encountered prior to the measurement; if there is not enough time, the measurement defaults to a GCP sighting. The primary difference between the two modes of operation is that prior to exiting from the sequencer, an interrupt is sent via a parallel data bus to a separate task hosted on the PDP 11/70 which simulates the sensor system and the operation of the registration processor.

V. GCP ANALYSIS

For the purpose of this study, the spacecraft orbit was assumed to be circular with an inclination to the equatorial plane at 80 degrees. For ease of setup and interpretation of results, the beginning of each simulation run was taken to be at a positive ascending mode with the inertial coordinate frame coincident with the earth's coordinate frame. This does not detract from the generality of the results since specific scenes on the surface or specific star catalogs were not used in the simulation.

A. ERROR BUDGET

1. Attitude Reference Unit

The attitude reference unit for this simulation was assumed to be of the NASA standard type (DRIRU II). It consists of three nominally orthogonal gyros whose characteristics are fairly well documented. The specifications for these gyros were studied and the terms applicable to the assumed system configuration and environment were used. The parameters specified and used are outlined in Table V-1.

2. Star Trackers

Each of the two star trackers assumed to be on board the vehicle are of the NASA standard type. For the purposes of this simulation, the optical axes of the two devices were assumed to be orthogonally oriented in a plane containing the vehicle position vector and perpendicular to the vehicle velocity vector. Documentation, including the OADS and existing specifications, was studied and the error terms felt to be applicable to this configuration and environment were used. These parameters are outlined in Table V-2.

Table V-1 Attitude Reference Unit Error Coefficients

Parameter	Value of Conventional Units, 1σ	Value Used, 1σ	Source
Gyro Long-Term Bias Uncertainity	0.017 deg/h	0.08×10^{-6} rad/s	Spec
Scale Factor Uncertainty	90 ppm	90.0×10^{-6}	Spec
Nonorthogonality of Mounting	2 arc-s	10×10^{-6} rad	Assumed
Package Alignment Uncertainty Relative to Mounting Surface Each Axis	10 arc-s	50×10^{-6}	Assumed
Gyro Noise Equivalent Angle	1.3 arc-s	10×10^{-6} rad/s	Spec
Absolute Bias	2 deg/h	10×10^{-6} rad/s	Spec
Absolute Scale Factor	0.5%	0.005	Spec

Table V-2 Star Tracker Error Coefficients

Parameter	Value of Conventional Units, 1σ	Value Used, 1σ	Source
Bias, Each Axis	10 arc-s	50×10^{-6} rad	Spec
Quantization	1 arc-s	5×10^{-6} rad	OADS
Misalignment Each Axis	5 arc-s	25×10^{-6} rad	OADS
Star Catalog	1 arc-s	5×10^{-6} rad	OADS

3. Global Positioning System (GPS)

The GPS is assumed to be available to the spacecraft virtually continuously. The update interval using GPS was predominantly 5 seconds; however, variations have been made in this parameter to study its affect on system performance. The GPS system error parameter assumed for the purposes of this simulation are presented in Table V-3.

Table V-3 GPS Error Coefficients

Parameter	Value of Conventional Units, 1σ	Value Used, 1σ	Source
Velocity Bias	0	0	Assumed
Velocity Noise	0.006 m/s	6×10^{-6} km/s	Assumed
Position Bias	0.04 m	4×10^{-5} km	Assumed
Position Noise	4.0 m	4×10^{-3} km	Assumed

4. **Landmark Tracker (LMT)**

The LMT was assumed to have its optical axis colinear with the nadir pointing axis of the spacecraft. The look angle to the landmark is in the plane containing the optical axis, perpendicular to the vehicle velocity vector. It has a maximum value of 10 degrees with two modes of operation. These modes are user-selectable to take on either fixed specified look angles or uniformly distributed look angles of a specified maximum magnitude. Table V-4 outlines the error characteristics assumed for the LMT.

Table V-4 Landmark Tracker Error Coefficients

Parameter	Value Conventional Units 1 σ	Value Used 1 σ	Source
Bias, Each Axis	2 arc-s	10×10^{-6} rad	Assumed
Quantization Each Axis	1 arc-s	5×10^{-6} rad	Assumed
Misalignment (three axes)	5 arc-s	25×10^{-6} rad	Assumed
Landmark Location Uncertainty	1 arc-s	5×10^{-6} rad	Assumed

B. PARAMETRIC STUDIES

The intent of the parametric studies was to determine the system's sensitivity to such parameters as LMT update interval, look angle mode and range, GPS update interval and accuracy, and recovery time after a long period without LMT Updates with and without star tracker backup. The study was progressive in the above order using as parameters the values that appeared to be optimum from the previous study. With the exception of the study of system sensitivity to the GPS accuracy, the error budget referred to was used uniformly for all studies.

Table V-5 outlines the cases studied by title and most significant parameters.

Table V-5 Cases Studied

Title	GCP Update Interval, s	GPS Update Interval, s	Remarks
GCP Update Interval Sensitivity			
CASE 1	5	5	CASE 1 through CASE 7 were run with ±10-deg random look angles as well as a 0-degree fixed look angle.
CASE 2	10	5	
CASE 3	20	5	
CASE 4	40	5	
CASE 5	80	5	
CASE 6	160	5	
CASE 7	320	5	
Look Angle Sensitivity			
CASE 9	80	5	0-deg fixed look angle.
CASE 10	80	5	2.5-deg fixed look angle.
CASE 12	80	5	5-deg fixed look angle.
CASE 14	80	5	10-deg fixed look angle.
CASE 17	80	5	±2.5-deg random look angle.
CASE 18	80	5	±5-deg random look angle.
GPS Sensitivity Update Interval			
CASE 21	80	10	CASE 21 through CASE 26 were run with ±10-deg look angles.
CASE 22	80	20	
CASE 23	80	40	
CASE 24	80	80	
Accuracy			
CASE 25	80	5	GPS velocity error increased by 4X.
CASE 26	80	5	GPS position error increased by 4X.
Recovery Sensitivity			
CASE 30	80	5	±10-deg random look angles; linear cloud table; default to star trackers.
CASE 31	80	5	±10-deg random look angles; GCP shut down for 1000 s with default to star trackers.
CASE 32	80	5	±10-deg random look angle; GCP shut down for 1000 s without default to star trackers.

C. SUMMARY OF RESULTS

The system as simulated met the requirements established earlier for conditions where the GCP update intervals are between 20 and 80 seconds with GPS updates taken at about 10-second intervals. In some cases part of the initial transient was included in estimation of the peak or 3σ value for a given parameter. Therefore most of the results are felt to be pessimistic with respect to the size of the error bounds. These results do not reflect the estimation of such gyro parameters as gyro bias, misalignment, scale factor error and nonorthogonality. With estimation and compensation for these parameters, the results should be further improved.

These studies took advantage of the fact that the reference body coordinate system is defined within the landmark tracker or GCP sensor. Therefore the misalignment of that sensor is by definition equal to zero. However, this shifts the error contribution of misalignment of other sensors if such misalignments are not estimated and compensated. The effects of such uncompensated terms as gyro bias may be seen in cases where long GCP update intervals are used. Further studies should be undertaken to implement the estimation and compensation of constant gyro parameters and possibly the landmark tracker parameters of bias and misalignment should that sensor coordinate frame not be taken as a body reference.

VI. CONCLUSION AND RECOMMENDATIONS

A. CONCLUSIONS

One of the key bottlenecks associated with NASA's end-to-end data management problem is the process of image correction. Resampling not only requires a tremendous amount of data processing but also requires the integration of volumes of data from every aspect of the mission, including gyro data, tracking data, and imagery.

With the development of the MLA, autonomous real-time image correction will become feasible. The distortions associated with the multispectral scanner's nonlinear mirror sweep and nonuniform sweep period will be eliminated, leaving a well-defined distortion caused by earth curvature and look angle. The tremendous increases in computational capabilities both on the ground and aboard the spacecraft will also simplify the problem.

A solution to the problem may be realized through either ground processing or spaceborne processing. However, even though ground-based processing may alleviate the immediate problem, in the long range adaptive systems using onboard intelligence will be required. Therefore it may be advantageous to begin the transition to onboard automated systems now.

In the past there has been a lack of coordination between the scientific user community and the engineers responsible for spacecraft design. This has resulted in a physical separation between the design and implementation of the science payload and the control system. An example of this thinking is shown in the multimission spacecraft (MMS) where subsystems are treated as modules and the payload itself is physically separated from the control portion of the vehicle. This type of design, although attractive from a standardization point of view, ignores the inherent relationships between user requirements, spacecraft control requirements, and ground support requirements. It is possible that rather than saving significant costs, standardization may result in higher end-to-end costs. This design philosophy must be reevaluated with regard to future missions. In the end-to-end design of remote sensing spacecraft, the primary emphasis in the guidance and control system must shift from simply estimating the ephemeris and attitude of the spacecraft to estimating the position of the science sensor's FOV on the earth's surface. This provides the basis for both real-time image correction and deterministic data acquisition through sensor pointing. This shift of emphasis will impact the design of the entire spacecraft. For example, if the science sensor boresight position is to be determined, it is desirable to place the gyro package close to that sensor to reduce the misalignment between the two. This (MMS) configuration, which provides a physical separation between the payload and the guidance and control system, may not satisfy the requirements of many future remote sensing missions.

Many benefits may be realized through onboard spacecraft control. By isolating the science sensor from the attitude limit cycle of the vehicle using a pointing mount, a curved focal plane MLA that provides uniform sampling of the image can be incorporated, thus reducing the

amount of resampling required. This approach, although attractive for missions such as Landsat where the revisit cycle is periodic, may not be attractive for missions requiring deterministic data acquisition through sensor pointing because a curved focal plane array boresight must always point at nadir. However, a pointing mount is useful in either case to isolate the science sensor from the attitude limit cycle.

One of the keys to future remote sensing missions is the onboard determination of sensor boresight position in earth-fixed coordinates. Both image correction and deterministic data acquisition systems will require this knowledge to be useful. Analysis has shown that inertial systems alone do not provide sufficient accuracy for several reasons:

1) It is difficult to resolve misalignments between inertial sensor frames and science sensor frames;

2) Misalignment between inertial and local earth frames are difficult to compute;

3) Star trackers are not accurate enough.

Ground control point (GCP) sightings can be used to directly solve for these misalignments and hence reduce the error in boresight determination.

Analysis has shown that a registration accuracy of 0.1 pixels can be achieved using an SSDA correlation algorithm. It is also possible to detect situations where the correlator locks onto a false target. These factors make the correlator an attractive navigation sensor for an onboard image correction system.

A system comprising two NASA standard star trackers, a NASA standard gyro package, a GPS receiver, and the landmark tracker with a 30-meter resolution was simulated. Analysis results indicate that with a GPS update frequency of between 5 and 10 seconds and a GCP sighting frequency of between 20 and 80 seconds, the position of the sensor boresight can be determined to within 15 meters. With the one exception of the MLA, the entire system can be implemented with existing technology. The most restricting feature of the system is the tremendous storage requirements for the GCP data base. Assuming that GCP's may only be located on land (accounting for 20% of the earth's surface) and assuming a GCP update frequency every 40 seconds or approximately every 1 1/3 scenes, the total storage requirements may be found by:

Total earth surface area $= 4-(6 \times 10^3)^2 \text{ km}^2$

$= 4.5 \times 10^8,$

Total number of available scenes $= 4.5 \times 10^8 \text{ km}^2 \times 0.2 \quad 175^2 \text{ km}^2$

$= 2.9 \times 10^3,$

Total number of GCPs $= 2.9 \times 10^3 \times 3/4$

$= 2 \times 10^3,$

Total memory required $= 2 \times 10^3 \text{ GCPs} \times 32^2 \ \frac{\text{pixels}}{\text{GCP}} \times \frac{8 \text{ bits}}{\text{pixel}} = 18 \times 10^6$ bits.

Although this is a tremendous storage requirement, it is still within the limits of current technology This volume may also be reduced by a factor of two by reducing the number of gray scales used in the reference GCP from 256 to 16. If histogram equalization is used to reduce the number of gray scales, the accuracy of the correlation may not be affected. This possibility should be investigated.

It is estimated that processing requirements can be met with the use of two general-purpose flight computers and a hardwired correlator. The separation of functions would be directly analogous to the navigation and the registration processors discussed in Section II.

B. RECOMMENDATIONS

If the landmark tracker is to be realized as an operational system, a well-planned development schedule is required. The critical tasks that must be performed include:

1) Further analysis of the correlator is required to determine its sensitivity to seasonal variations. It is also necessary to determine the types of landmarks that produce the best correlation. This information will be invaluable in the selection of GCPs for an operational system;
2) Research must be conducted to determine methods of reducing the storage requirements of the GCP data base. The most promising approach seems to be a mixture of image enhancement and gray scale reduction;
3) A study must be conducted to establish the configuration of the onboard processing network;
4) The entire system should be breadboarded and ground-tested to resolve peculiarities of the design;
5) The breadboard system may be flown on a low-cost aircraft flight test to more fully demonstrate feasibility;
6) The breadboard system could also be incorporated into the IAS ground demonstration as an additional step toward a total system configuration.

The curved focal plane MLA is another concept that should be investigated. If feasible, the concept would dramatically reduce the processing requirements associated with remote sensing missions. This investigation can be separated into two tasks. First, the feasibility of the concept must be analyzed. Technical considerations include:

1) Precision required in machining of the curved surface;
2) Effect of variations in local earth curvature on registration accuracy;
3) Pointing requirements needed to ensure 1/2 pixel registration.

The second task that must be performed is a cost/benefit tradeoff between deterministic data acquisition through sensor pointing versus image correction using the curved focal plane array. The two approaches are mutually exclusive.

VII. REFERENCES

1. Space Systems Technology Model. National Aeronautics and Space Administration Office of Aeronautics and Space Technology, Code RS, NASA Headquarters, Washington, DC, May 1980.

2. P. C. Carney et al.: Onboard Attitude Determination System Final Report, NAS4-23428 Mod. 27, Martin Marietta Denver Aerospace, 1978.

3. H. M. Thomas et al.: Definition of Second Feature Identification and Location Experiment (FILE-II). MCR-81-539, Prepared under Contract NAS1-15737, March 1981.

4. R. L. White et al.: "Attitude and Orbit Estimation Using Stars and Landmarks." IEEE Transactions on Aerospace and Electronic Systems, Vol AES-11, No. 2, 1974.

5. R. L. White et al.: "Use of Known Landmarks for Satellite Navigation." AIAA Paper No. 75-1097, 1975.

6. N. F. Toda and F. H. Schlee: "Autonomous Orbital Navigation by Optical Tracking of Unknown Landmarks." Journal of Spacecraft and Rockets, Vol 4, No. 12, 1967.

7. D. H. Aldrich: "Interferometer Landmark Tracker Navigation System." Neacon Journal, 1974.

8. D. I. Barnea and H. F. Silverman: "A Class of Algorithms for Fast Digital Image Registration." IEEE Transactions on Computers, Vol C-21, No. 2, February, 1972.

9. R. T. Schappell et al.: Experimental and Simulation Study Results for Video Landmark Acquisition and Tracking Technology. NASA Contractor Report 158997 prepared under Contract NAS1-14489, February 1979.

10. L. E. Gilbert et al.: "Onboard Landmark Navigation and Attitude Reference Parallel Processor System." Paper presented at the Second Annual Flight Mechanics and Estimation Theory Symposium, 1977.